NIH Public Access
Author Manuscript
Cell Rep. Author manuscript; available in PMC 2015 June 12.

Published in final edited form as:
Cell Rep. 2014 June 12; 7(5): 1614–1625. doi:10.1016/j.celrep.2014.04.054.

A Role for Stargazin in Experience-Dependent Plasticity

SR Louros[1,2,3], **BM Hooks**[3], **L Litvina**[3], **AL Carvalho**[2,4,**], and **C Chen**[3,*]

[1]Ph.D. Program in Experimental Biology and Biomedicine, Center for Neuroscience and Cell Biology, University of Coimbra, Portugal

[2]Center for Neuroscience and Cell Biology, University of Coimbra, 3004-504, Coimbra, Portugal

[3]F.M. Kirby Neurobiology Center, Children´s Hospital, Boston, Harvard Medical School, 300 Longwood Avenue, Boston, MA 02115, USA

[4]Department of Life Sciences, University of Coimbra, 3001-401, Coimbra, Portugal

Summary

During development neurons are constantly refining their connections in response to changes in activity. Experience-dependent plasticity is a key form of synaptic plasticity, involving changes in α-amino-3-hydroxy-5-methyl-4-isoxazolepropionic acid receptor (AMPAR) accumulation at synapses. Here we report a critical role for the AMPAR auxiliary subunit, stargazin, in this plasticity. We show that stargazin is functional at the retinogeniculate synapse and that in the absence of stargazin, the refinement of the retinogeniculate synapse is specifically disrupted during the experience-dependent phase. Importantly, we found that stargazin expression and phosphorylation increased with visual deprivation, and led to reduced AMPAR rectification at the retinogeniculate synapse. To test whether stargazin may play a role in homeostatic plasticity, we turned to cultured neurons and found that stargazin phosphorylation is essential for synaptic scaling. Overall, our data reveal an important new role of stargazin in regulating AMPAR abundance and composition at glutamatergic synapses during homeostatic and experience-dependent plasticity.

Introduction

Proper wiring of neural circuits during development depends on both molecular cues that guide connectivity and activity-dependent mechanisms that adjust the strength and number of synaptic connections. One powerful experimental system for studying these processes is the murine visual system. For example, the retinogeniculate synapse, the connection between retinal ganglion cells and relay neurons in the dorsal lateral geniculate nucleus (LGN) of the thalamus, exhibits well characterized phases of plasticity and circuit

© 2014 Elsevier Inc. All rights reserved.

*To whom correspondence should be addressed: chinfei.chen@childrens.harvard.edu, ph: 617-919-2685; fax: 617-919-2777.
**alc@cnc.uc.pt, ph: +351-304-502-610; fax: +351-239-822-776.

Publisher's Disclaimer: This is a PDF file of an unedited manuscript that has been accepted for publication. As a service to our customers we are providing this early version of the manuscript. The manuscript will undergo copyediting, typesetting, and review of the resulting proof before it is published in its final citable form. Please note that during the production process errors may be discovered which could affect the content, and all legal disclaimers that apply to the journal pertain.

NIH-PA Author Manuscript
NIH-PA Author Manuscript
NIH-PA Author Manuscript

NIH-PA Author Manuscript

NIH-PA Author Manuscript

NIH-PA Author Manuscript

maturation (Hong and Chen, 2011). After the initial mapping of RGC axon terminals to their target, a phase of synapse elimination and strengthening that depends on spontaneous activity, not vision, results in a rough draft of the final circuit configuration. This phase is followed by a critical period during which visual experience further refines and stabilizes the mature circuit. Visual deprivation during this later phase (P20, late dark rearing, LDR) results in weakening of the average RGC input and recruitment of additional afferents. In contrast, chronic dark rearing (CDR) from birth does not elicit major synaptic rearrangements (Hooks and Chen, 2006).

The mechanisms that underlie remodeling of the thalamic circuitry in response to LDR are not well understood. Hebbian processes are thought to contribute to spontaneous activity-dependent plasticity during retinogeniculate development (Butts et al., 2007; Krahe and Guido, 2011; Ziburkus et al., 2009). However, the increase in afferent innervation in LDR mice suggests that homeostatic mechanisms could play a role in experience-dependent plasticity. In response to alterations in neuronal activity, homeostatic plasticity maintains the stability of the network activity within a dynamic range for effective information transfer (Turrigiano, 2008). Importantly, manipulation of visual experience *in vivo* has been shown to induce homeostatic adjustments in other regions of the visual system (Chandrasekaran et al., 2005; Chandrasekaran et al., 2007; Desai et al., 2002; Krahe and Guido, 2011; Maffei and Turrigiano, 2008). Consistent with a role for homeostatic mechanisms in experience-dependent plasticity, recent studies have demonstrated the importance of MeCP2, a transcriptional regulator associated with Rett Syndrome, in synaptic scaling *in vitro* (Qiu et al., 2012; Zhong et al., 2012) and in the visual cortical scaling up in response to visual deprivation (Blackman et al., 2012). Studies from our own lab have demonstrated that MeCP2 plays an essential role in experience-dependent plasticity at the retinogeniculate synapse (Noutel et al., 2011). Yet how homeostatic plasticity mediates synaptic remodeling *in vivo* and *in vitro* is still not clear.

Because AMPARs are central to the plasticity of connections in the LGN, dynamic regulation of these receptors must be essential for experience-dependent circuit rewiring. Thus we examined the involvement of stargazin, an auxiliary subunit of AMPARs that regulates their delivery to the synapse (Chen et al., 2000; Opazo et al., 2010). Here we describe essential roles of stargazin phosphorylation in both synaptic scaling and experience-dependent plasticity.

Results

Stargazin is essential for retinogeniculate synapse remodeling

Developmental remodeling at the retinogeniculate synapse is notable for the robust synapse strengthening during normal development as well as the change in strength and connectivity that occurs in response to visual deprivation. In both cases, the regulation of AMPAR presence in the postsynaptic densities must be critical for rewiring the circuit. Many molecules have been associated with AMPAR, including the Transmembrane AMPA Receptor Regulatory Proteins (TARPs). The protein stargazin (STG) is one of the best characterized proteins of this class, and thus we first asked whether this TARP plays a role in retinogeniculate synapse remodeling. To determine whether STG is expressed in the

NIH-PA Author Manuscript

NIH-PA Author Manuscript

NIH-PA Author Manuscript

LGN, we dissected LGNs from acute mouse brain slices at different ages and looked at total STG expression by western blot. The antibody used in this study recognizes a 37kDa band that is absent in stargazer mice that lack STG expression (Letts et al., 1998), confirming this band as STG (Fig. 1A). In wildtype (WT) mice STG protein levels in the LGN increase after P10, reaching maximal levels of expression after P15, a developmental timepoint just after eye opening (P12) (Fig. 1B,C). STG expression remains elevated at P27–32, when synaptic strength has reached the mature level (P=0.03, t-test, P10 compared to P27).

The LGN contains two classes of neurons, the excitatory relay neurons that project to the visual cortex and intrinsic inhibitory neurons. While both classes of neurons receive retinal inputs, relay neurons outnumber interneurons by 4:1 (Ohara et al., 1983). To test whether STG plays a role specifically at retinogeniculate synapses, we examined the stargazer mouse. We found that the AMPAR/NMDAR current ratio was reduced at all ages in stargazer when compared to their WT littermates, consistent with a role for STG in AMPAR insertion at the synapse (Fig. 1D, E). The deficit is most severe in older mice (AMPA/NMDA ratio of 1.22 vs. 0.82 at P27–32, $P<0.001$, ANOVA, Bonferroni test). Despite the lack of STG, however, the ratio increased from 0.40 to 0.82 between P15 and P32 in stargazer mice ($P<0.01$ ANOVA, Bonferroni test). This suggests that other AMPAR-interacting proteins are also responsible for AMPAR insertion at retinogeniculate synapses (Fukaya et al., 2005; Payne, 2008). Indeed, we detected TARPγ4 expression in LGN with a similar developmental expression pattern as STG (Fig. S1A), which may explain the persistence of synaptic AMPARs in stargazer mice (Tomita et al., 2003). However, we did not detect a change in TARPγ4 expression levels in the LGN of stargazer mice relative to WT (Fig. S1B). These results clearly implicate STG in the trafficking and insertion of AMPAR at the retinogeniculate synapse.

If STG is involved in AMPAR trafficking into the retinogeniculate synapse, it could play a role in the developmental refinement of this circuit. We compared the single fiber strength and number of afferent inputs onto relay neurons in stargazer and WT littermates. Fig. 2 shows representative examples of AMPAR and NMDAR mediated currents from WT (A) and stargazer (B) littermates in response to increasing stimulus intensities at P15–16 (top) and P27–32 (bottom). Consistent with previous reports, the evoked synaptic currents in stg−/− mice differed from that of stg+/+ mice in their AMPAR/NMDAR ratio (Fig. 2A,B) (Lacey et al., 2012; Menuz and Nicoll, 2008). However, at P15–16, the average AMPAR and NMDAR single fiber current amplitude were similar for the two genotypes (for AMPAR, Fig. 2C). To estimate the number of afferent inputs we calculated the fiber fraction ratio, which quantifies the fractional contribution of that input to the maximum current of a given cell (Hooks and Chen, 2006). Fiber fraction ratio was not changed in the absence of stargazin at P15–16 (Fig. 2D). Similarly, analysis of retinogeniculate connectivity at P19–21 revealed no significant differences in single fiber strength (data not shown, Mann Whitney test: P=0.1, n=29–31) or fiber fraction (Fig. 2D). However, after the vision-dependent phase of synaptic remodeling (between P20–P34), differences between WT and mutant mice became evident: single fiber AMPAR EPSC amplitudes were significantly smaller in stg−/− mice as shown by the leftward shift in the cumulative probability amplitude distribution at P27–32 (Fig. 2C, right; KS test: P=0.003). Moreover, fiber fraction was significantly reduced in stg−/− mice, consistent with an increased number of afferent inputs (0.29±0.04,

NIH-PA Author Manuscript

NIH-PA Author Manuscript

NIH-PA Author Manuscript

n=70 in WT p27–32, compared to 0.19 ± 0.03, n=88 in stg−/− mice; Fig. 2D). Therefore, even in the absence of STG, retinogeniculate synapses strengthen and refine during the spontaneous activity-dependent phase development (<P20). However, synaptic connectivity becomes significantly disrupted later in development, during the vision-sensitive period of the thalamic circuit.

Stargazer mice exhibit frequent absence-like seizures (Burgess and Noebels, 1999), raising the possibility that pre-P20 seizures may disrupt experience-dependent synaptic refinement. To test this possibility, we examined synaptic maturation in another mouse seizure model, the Tottering mouse. In Tottering, a mutation in the P/Q-type HVA voltage-gated calcium channel subunit α1A (Cacna1a) leads to a similar phenotype as stargazer, with onset of absence-like seizures by P15 (Burgess and Noebels, 1999). Figure S2 shows that in contrast to stg−/− mice, refinement in Tottering mice is normal at P27–32. Therefore, increased excitability of thalamic circuits from absence-like seizures, *per se*, does not disrupt retinogeniculate refinement. Taken together, these results point to a specific role of STG in experience-dependent synaptic remodeling.

Stargazin expression is regulated by visual experience

To test whether STG is regulated by experience, we compared the expression levels of STG in C57BL/6J mice exposed to different visual manipulations. We have previously demonstrated that visual deprivation from birth (CDR) does not elicit changes in synaptic connectivity, whereas dark-rearing for one week at P20 (LDR) elicits robust rearrangements of the retinogeniculate synapse, weakening single fiber strength and increasing the number of afferent inputs (Hooks and Chen, 2006, 2008). STG levels significantly increased in the LGN of LDR but not CDR mice (Fig. 3A,B; P=0.03 for STG levels in LDR compared to light reared (LR) mice, ANOVA followed by Dunnett's test). In contrast, the expression of TARPγ4 was not changed by either visual manipulation (Fig. 3C,D, n=3, P=0.63, ANOVA), consistent with an important role of STG in the remodeling of the retinogeniculate synapse during LDR.

The function of STG is regulated by the phosphorylation of nine consecutive serine residues in the cytoplasmatic tail of the protein; this phosphorylation regulates the interaction of STG with PSD-95 (Tomita et al., 2005). STG commonly migrates as a doublet on denaturing SDS-PAGE conditions and this correlates with the phosphorylation state of the protein (see Fig. S3A and (Tomita et al., 2005)). Consistent with phosphorylated STG in the LGN, we found that lambda-phosphatase treatment of LGN lysates selectively removed the upper, putatively phosphorylated band of the doublet (Fig 3E). We hypothesized that STG phosphorylation is altered in conditions that trigger experience-dependent plasticity, thus we analyzed relative levels of STG phosphorylation in LR, CDR and LDR mice using a phospho-specific antibody to two consecutive serine residues, S239/S240 (Fig. S3B). We found a significant increase in STG phosphorylation in LDR mice when compared to LR mice (40 ± 13% P=0.015 ANOVA followed by Dunnett's test, Fig. 3F,G). These findings are consistent with the active regulation of STG phosphorylation by change in vision in relay neurons of the LGN.

NIH-PA Author Manuscript

NIH-PA Author Manuscript

NIH-PA Author Manuscript

Stargazin modifies AMPAR EPSCs at the retinogeniculate synapse

If STG mediates retinogeniculate synapse remodeling in an experience-dependent manner, we might be able to monitor this process functionally. STG modifies the AMPAR I-V relationship such that there is increased rectification at positive holding potentials. Two distinct roles of STG in AMPAR rectification have been described. In cerebellar neurons from stargazer mice, intracellular retention of the GluA2-containing calcium-impermeable (CI-)AMPAR (Tomita et al., 2003) leads to increased synaptic accumulation of inwardly-rectifying calcium-permeable (CP-AMPAR) channels (Bats et al., 2012; Yamazaki et al., 2010, Hollmann et al., 1991). Because CI-AMPAR present a linear I-V relationship, changes in the composition of AMPAR subunit types at synapses can be monitored functionally by analyzing the AMPAR rectification index (RI; the ratio between the current amplitude at negative potentials to that at positive potentials). Other studies have also demonstrated that STG attenuates AMPAR polyamine block (Soto et al., 2007), which could account for the differences detected in the rectification of AMPAR in stargazer mice.

We analyzed EPSC rectification properties at the retinogeniculate synapse by recording AMPA-mediated currents at different voltages, in the presence of saturating concentrations of intracellular spermine (100 μM), which produces a voltage-dependent block of calcium-permeable (CP)-AMPARs. We found that at P27, AMPAR-mediated currents are more rectified in stargazer mice (P=0.002, t-test), suggesting increased contribution of CP-AMPARs (Fig. 4A,B).

We next asked whether a change in the level of STG in the LGN of LDR mice also altered AMPAR current rectification at the retinogeniculate synapse. We compared the rectification properties of the retinogeniculate AMPAR EPSC in visually manipulated mice (Fig. 4C,D). Consistent with a role for STG in experience-dependent synapse remodeling, CDR did not affect AMPAR rectification but LDR reduced the RI (I_{-60mV}/I_{+40mV}, Fig. 4D, P=0.007, ANOVA followed by Bonferroni test, LDR compared to LR). Our results demonstrate that STG is present and functional at the retinogeniculate synapse during the vision-sensitive period.

In the LGN, GluA1 is inserted at the retinogeniculate synapse in a vision-dependent manner (Kielland et al., 2009). To test whether this process might explain the reduction in AMPAR RI of LDR mice, we examined expression levels of GluA1 and GluA2 subunits in the LGN. Figure 4E,F demonstrates a significant increase in GluA2/GluA1 ratio in the LGN of LDR (P=0.03, LDR compared to LR, ANOVA followed by Dunnett's test) consistent with higher expression of CI- AMPAR at the retinogeniculate synapse. These results suggest that STG controls AMPAR trafficking and insertion at the retinogeniculate synapse after P20, supporting the model that STG is required for proper remodeling of the retinogeniculate synapse during the vision-sensitive period.

Stargazin mediates synaptic scaling

Given that synaptic remodeling in the retinogeniculate synapse is triggered by change in visual activity (Hooks & Chen, 2006) and that LDR increases maximum AMPAR-evoked currents, we hypothesized that homeostatic adaptation in response to lack of visual

NIH-PA Author Manuscript

NIH-PA Author Manuscript

NIH-PA Author Manuscript

experience occurs in LDR. Further testing of whether STG mediates experience-dependent homeostatic plasticity *in vivo* was hampered by the fact that the retinogeniculate synapse is part of a larger thalamic circuit in which other connections have been shown to be dependent on STG (Lacey et al., 2012; Menuz and Nicoll, 2008). It was difficult to assess homeostatic responses at one synapse without considering changes at other synapses in the circuit. For this reason we turned to a simpler culture system where STG expression could be manipulated in neurons that are innervated by WT inputs. We chose the cortical culture system as it is an established model for studying homeostatic plasticity, and in particular, synaptic scaling. Synaptic scaling is a form of homeostatic plasticity by which neurons adjust their synaptic strength by changing AMPAR content at excitatory synapses in order to maintain stable neuronal output during alterations in network activity (Turrigiano, 2008).

Low-density cortical neurons were treated for 48h with the voltage-gated Na^+ channel blocker tetrodotoxin (TTX, 1 μM) to block action potential generation, and surface AMPAR content was quantified by incubating live neurons with an antibody specific to the N-terminus of the GluA1 subunit (Fig. 5A). As previously described (Wierenga et al., 2005), TTX treatment significantly increased total surface GluA1 cluster fluorescence intensity, area and number in cortical neurons ($P<0.0001$ significantly different from CTR, t-test, Fig. 5B). Synaptic GluA1, defined as GluA1 puncta that co-localized with an excitatory postsynaptic marker, PSD95, was also quantified. Chronic treatment with TTX also increased the intensity ($P=0.0007$, t-test), area ($P=0.0002$, t-test) and number ($P=0.009$, t-test) of synaptic GluA1 clusters (Figure 5B). To confirm that the scaling of GluA1 synaptic accumulation was multiplicative, a defining characteristic of synaptic scaling, we plotted ranked control GluA1 synaptic cluster intensities against ranked TTX GluA1 synaptic cluster intensities. The data were well fit by a linear function with a slope of 2.6 (Fig. 5C1), a multiplicative factor similar to that reported in the initial description of synaptic scaling (Turrigiano et al., 1998). The cumulative distribution of the data acquired from TTX incubated neurons scaled by this multiplicative factor is almost completely superimposable over the distribution of data from control neurons (Fig. 5C2). These results were consistent with previous reports of TTX-induced global synaptic up-scaling, and demonstrated that we could detect synaptic scaling by quantifying synaptic surface GluA1 by immunocytochemistry in low-density cortical neurons.

We next analyzed STG expression in TTX-stimulated cortical neurons and found a significant increase in total STG levels corresponding to homoestatic up-regulation of AMPAR (Fig. 5D,E; $P<0.01$, t-test). We also analyzed the localization and accumulation of endogenous STG along dendrites by immunofluorescence (Fig. 5F). Chronic blockade of neuronal activity with TTX resulted in an accumulation of STG along dendrites, as quantified by an increase in intensity ($P<0.0001$, t-test), area ($P<0.0001$, t-test) and number ($P=0.003$, t-test) of STG clusters (Fig. 5G). Moreover, TTX stimulation increased the intensity ($P=0.0003$, t-test) and area ($P=0.0002$, t-test) of STG clusters at synaptic sites (Fig. 5H), suggesting a role of STG in AMPAR trafficking during synaptic scaling.

NIH-PA Author Manuscript

NIH-PA Author Manuscript

NIH-PA Author Manuscript

Stargazin is essential for synaptic scaling

To test whether STG is required for synaptic scaling, we knocked down STG in sparse cultured cortical neurons using a shRNA sequence against STG mRNA in the pLentiLox3.7(CMV)EGFP vector. shRNA#4 efficiently decreased the intensity of STG immunolabeling to 32.2 ± 3% of endogenous levels (Fig. 6B,D; $P<0.0001$, t-test). To investigate the effect of STG knockdown in synaptic scaling, we treated cultured cortical neurons transfected with control shRNA (mock) or STG shRNA#4 with TTX for 48h, and live stained the cultures for cell surface GluA1 (Fig. 6D). In control conditions STG knockdown caused a 48.4 ± 5% decrease in total surface GluA1 levels (Fig. 6E); TTX treatment increased the cell surface GluA1 in mock-transfected cells ($P<0.001$, ANOVA followed by the Bonferroni test), but not in cells expressing shRNA#4 (Fig. 6E). Importantly, synaptic scaling could be restored by the expression of an shRNA-resistant form of STG (Fig. 6E; $P<0.01$, ANOVA followed by the Bonferroni test). These results demonstrate that STG is essential for synaptic scaling.

Stargazin phosphorylation is required for synaptic scaling

CaMKII and PKC can phosphorylate STG at nine serine residues of its intracellular C-terminal tail (Tomita et al., 2005). STG phosphorylation has been implicated in Hebbian forms of synaptic plasticity (Tomita et al., 2005) and in the diffusional trapping of AMPAR at synaptic sites due to increased interaction with PSD95 (Opazo et al., 2010). We found that prolonged inactivity induced by TTX treatment significantly increased activation of PKC (Fig. S4A,B) and phosphorylation of CaMKIIβ but not of CaMKIIα (Fig. S4C,D), consistent with previous reports implicating this isoform in synaptic scaling (Groth et al., 2011; Thiagarajan et al., 2002). To test whether STG phosphorylation was affected with TTX treatment we looked at the phosphorylation of three serines (S228 and S239/240) using phospho-specific antibodies. Indeed, chronic activity blockade significantly increased STG phosphorylation at S239/240 ($P=0.005$ CTR vs. 48h, t-test) and S228 ($P=0.03$ CTR vs. 48h, t-test) (Fig. 7A,B). Interestingly, S239/240 phosphorylation increased within a few hours after TTX application, whereas the increase in S228 phosphorylation could only be detected 48h after TTX treatment. To further test whether STG phosphorylation mediates synaptic scaling, we co-transfected cortical neurons with GFP together with either WT stargazin or mutant forms of stargazin in which the nine serine phosphorylation sites were genetically altered (Fig. 7C). The nine serine residues are mutated to alanine in the phospho-dead mutant of STG (S9A) to mimic the dephosphorylated protein, or replaced by aspartate residues in the phospho-mimetic mutant of STG (S9D) to mimic the fully phosphorylated protein (Tomita et al., 2005). Consistent with previously described studies, overexpression of WT STG or S9A did not affect the baseline levels of surface or synaptic GluA1 (Fig. 7E), while overexpressing S9D increased the baseline levels of AMPAR at the surface of cortical neurons. If the regulation of STG phosphorylation is required for TTX-induced increase in surface GluA1 expression, we would expect to disrupt synaptic scaling when over-expressing STG mutants. Indeed, overexpression of STG phospho-dead mutant blocked AMPAR accumulation at synapses in response to TTX (Fig. 7E), indicating that STG phosphorylation is required for synaptic scaling. Moreover, overexpression of the phospho-mimetic mutant S9D occluded TTX-induced synaptic scaling (Fig. 7E). Altogether, these

NIH-PA Author Manuscript

NIH-PA Author Manuscript

NIH-PA Author Manuscript

results strongly support that STG phosphorylation is essential for the scaling of glutamatergic synapses.

The insertion of different subunits of AMPARs during homeostatic plasticity remains controversial and seems to be dependent on the model system or stimuli used to induce synaptic scaling (reviewed by (Lee, 2012)). To look at different AMPAR subunits at the surface of cortical neurons after synaptic scaling induction, we biotinylated and isolated cell surface proteins. Consistent with Fig. 7 we observed an increase in GluA1 surface accumulation upon chronic inactivity, but GluA2 subunit surface accumulation increased further, resulting in a 21.2 ± 2.8% increase in total GluA2/GluA1 ratio (P=0.017, t-test) and a 25.7 ± 2.3% increase in GluA2/GluA1 surface expression (Fig. S5; P=0.008, t-test). This may be due to an accumulation of both GluA1-GluA2 and GluA2-GluA3 heteromers at the surface of cortical neurons after 48h of inactivity. The over-expression of STG phospho-mutants differentially affected surface insertion of GluA1 and GluA2 subunits of AMPAR during chronic inactivity (Fig. S5C,D). We confirmed the results from our single-cell analysis (Fig 7E,F), where the expression of STG phospho-mutants blocked TTX-induced GluA1 increase at the surface of neurons (Fig. S5E). Interestingly, GluA2 subunit insertion was differentially affected by the expression of the two STG phospho-mutants (Fig. S5F) raising an interesting possibility that the phosphorylation of STG may influence the interaction of GluA2-containing receptors with other interactors, such as PICK1, previously implicated in scaling up (Anggono et al., 2011).

Discussion

In this study, we uncover a previously unrecognized role for STG in experience-dependent plasticity. We show for the first time that LDR, a manipulation that elicits a homeostatic-like remodeling of the retinogeniculate connection, regulates STG phosphorylation state and AMPAR composition. Phosphorylation of STG is necessary for scaling up of synaptic strength in TTX treated cortical neurons. Common features were found between chronic inactivity induced by TTX in cortical neurons and the retinogeniculate synapse properties after LDR in mice, with a significant up-regulation of STG and GluA2-containing AMPAR in both conditions. These findings suggest that phosphorylation of STG can mediate synaptic plasticity and remodeling during critical periods of sensory circuit development.

Phosphorylation of Stargazin regulates synaptic scaling

Previous studies have identified STG as a critical mediator of long-term synaptic plasticity (LTP and LTD). STG phosphorylation at nine serine residues is regulated by neuronal activity through the activation of PKC and CaMKII (Tomita et al., 2005). Phosphorylation of the TARP decreases STG-lipid interactions and enhances PSD95-STG interaction (Bats et al., 2007; Schnell et al., 2002; Sumioka et al., 2010), resulting in AMPAR immobilization at the PSD (Opazo et al., 2010) and synaptic strengthening. Through the phosphorylation and dephosphorylation of STG, synapse specific LTP and LTD can be regulated (Tomita et al. 2005). Here, we demonstrate that in addition to STG's role in Hebbian-like plasticity, STG phosphorylation is essential for synaptic up-scaling in response to chronic activity blockade. In cortical cultures, we found that STG phosphorylation was increased by chronic inactivity.

NIH-PA Author Manuscript

NIH-PA Author Manuscript

NIH-PA Author Manuscript

In addition, over-expression of STG phospho-mutants led to complete blockade or occlusion of synaptic scaling. It is important to note that the expression of the phospho-dead (S9A) mutant of STG did not affect AMPAR accumulation at synapses, arguing against the trivial explanation that the results are secondary to a disruption of AMPAR trafficking into the synapse. Instead, our data shows that phosphorylation of STG is essential for synaptic scaling in response to chronic activity blockade.

How STG phosphorylation differentiates between Hebbian and homeostatic plasticity is still unclear. Recent studies have suggested that the two forms of plasticity can interact. Conditions that silence neuronal activity can also enhance LTP (Arendt et al., 2013). Moreover, experience-dependent homeostatic adaptation in the visual cortex can be reversed through Hebbian plasticity mechanisms (Desai et al., 2002; Goel et al., 2006; He et al., 2007). Although both PKC and CaMKII play a role in synaptic scaling and LTP (Lisman et al., 2012; Malinow et al., 1988; Nicoll and Roche, 2013), signaling upstream of these enzymes or subcellular localization of activated PKC/CaMKII could be distinct. Other possibilities include a site-specific phosphorylation code and/or a temporal sequence in serine phosphorylation. The latter is an attractive model, supported by our findings that the time-course for phosphorylation of S239/S249 and S228 in STG is different in response to chronic inactivity, and is consistent with the finding that different phosphorylation sites regulate the binding of STG to other proteins (Matsuda et al., 2013). In the future, it will be interesting to test whether phosphorylation of specific serine residues distinguishes between the two fundamentally different forms of synaptic plasticity.

Regulation of Stargazin *in vivo* by visual experience

Classic *in vitro* studies of STG have provided great insight on how activity regulates AMPAR trafficking (Jackson and Nicoll, 2011). How physiological stimuli regulate STG *in vivo* is less clear. Here, we turned to the visual system, where developmental refinement of synaptic circuits is driven by both spontaneous and experience-dependent plasticity (Hong and Chen, 2011). We show that sensory experience can regulate STG expression and phosphorylation. Our data demonstrate that during the developmental period driven by spontaneous activity, STG is expressed in the LGN, and loss of STG disrupts the AMPAR/NMDAR ratios at the retinogeniculate synapse. STG expression levels increase during development in both normally reared and CDR mice. However, visually depriving mice during the experience-sensitive critical period further increased both STG levels and the phosphorylation of serine residues present at the C-terminal tail of STG. Consistent with a role for STG in this late phase of synapse remodeling, developmental convergence of afferent inputs is not disrupted until after P21 in stg−/− mice. During this phase, the reduced synaptic strength and apparent increase in afferent inputs is likely a result of high mobility of AMPAR in and out of synaptic sites in the absence of STG. Our results suggest that during normal light experience, STG phosphorylation is responsible for stabilization of the refined retinogeniculate connection.

Remarkably, the regulation of STG by visual experience occurred during a limited window of time. Shifting the onset of dark rearing by 5 days (DR from P25 to P32), a manipulation that does not induce remodeling at the retinogeniculate synapse (Delayed DR, Hooks and

NIH-PA Author Manuscript

NIH-PA Author Manuscript

NIH-PA Author Manuscript

Chen, 2008), also did not alter STG expression levels (Fig. S6). Moreover, the regulation of STG by sensory activity cannot be generalized to all TARPS; another TARP in LGN, γ4, was not sensitive to visual manipulations. Thus STG is a TARP that specifically mediates experience-dependent synaptic plasticity at this thalamic synapse. Based on our findings, we propose that different phases of retinogeniculate synapse maturation depend on distinct molecular pathways, with the phosphorylation of STG mediating the experience-dependent plasticity phase of remodeling.

AMPAR composition in Experience-Dependent Synapse Remodeling

Our results show that STG regulates AMPAR rectification at the retinogeniculate synapse during the late phase of development. Loss of STG increases AMPAR rectification, while increased expression of STG in response to LDR leads to a more linear I–V. Two mechanisms underlying STG's role in rectification have been described; one involves trafficking of specific AMPAR subunits into the synapse, and the other entails reducing the CP-AMPAR affinity to intracellular polyamines (Soto et al., 2007). We favor the former explanation at the retinogeniculate synapse, with STG trafficking more GluA2-containing AMPAR during LDR, for several reasons. First, we find an increase in the GluA2/GluA1 ratio in the immunoblots of LGN of LDR mice when compared to LR mice consistent with increased expression of GluA2-containing AMPAR at relay neurons. In addition, we detected intracellular accumulation of GluA2 subunit in LGN of stargazer mice by de-glycosylation analysis (data not shown), as previously shown for the cerebellum of stargazer mice (Tomita et al., 2003). Finally, the change in GluA2/GluA1 ratio in LDR is consistent with a previous report by Kielland et al, 2009 who found that while relay neurons in the visual thalamus receive glutamatergic inputs from both the retina and the cortex, GluA1 subunits are preferentially inserted into retinal synapses in response to visual stimulation. Interestingly, visual deprivation from birth (CDR) does not alter the I-V relationship in the same manner as LDR, supporting our hypothesis that turnover of AMPAR subunits occurs in response to changes in vision during a discrete period of time.

Our studies cannot distinguish whether STG preferentially traffics GluA2 over GluA1, as suggested by some reports (Tomita et al. 2003), or whether the composition of AMPAR is determined by the intracellular abundance of the subunit (Chen et al., 2000). It is also unclear whether the specific AMPAR subunit class is important for homeostatic plasticity at the retinogeniculate synapse. Regardless, we were able to monitor the effect of STG on AMPAR trafficking into the retinogeniculate synapse during the vision-sensitive period.

Homeostatic Plasticity and the Visual System

Homeostatic plasticity in response to changes in activity plays an important role in the development of the visual system (Maffei and Turrigiano, 2008). In the visual cortex, this form of plasticity occurs in response to visual deprivation during specific windows of development (Desai et al., 2002), and plays a role in ocular dominance plasticity (Kaneko et al., 2008; Mrsic-Flogel et al., 2007). Around the time of eye-opening, monocular deprivation can increase spontaneous corticothalamic activity (Krahe and Guido, 2011). In the superior colliculus, homeostatic mechanisms contribute to the conservation of total retinocollicular

NIH-PA Author Manuscript

NIH-PA Author Manuscript

NIH-PA Author Manuscript

input in response to disruption of spontaneous retinal wave activity (Chandrasekaran et al., 2005; Chandrasekaran et al., 2007).

Consistent with these studies, the synaptic response to LDR has many features of homeostatic plasticity. Synaptic remodeling is elicited by a change in vision—CDR does not exhibit plasticity even though sensory experience is the same as LDR between P20–34. Moreover, the recruitment in LDR of more afferent inputs offsets the reduction in single fiber strength and leads to an increase in maximal currents. Here, we present evidence that LDR-elicited retinogeniculate plasticity shares molecular pathways with *in vitro* synaptic scaling, showing for the first time that STG is regulated by vision in the LGN and that disrupting STG function interferes with experience-dependent remodeling of the retinogeniculate synapse. Based on these results, we propose that LDR elicits a homeostatic up-regulation of AMPAR in the retinogeniculate synapse. Increased STG expression and phosphorylation mediate the insertion of AMPAR into previously silent or weak synaptic sites throughout the relay neuron, resulting in a change in the number of afferent RGC inputs. Taken together, our data show an important role for STG phosphorylation in synaptic up-scaling and in sensory-dependent synapse remodeling.

Experimental procedures

Animals

Stg −/− and +/+ littermates and C57BL/6 mice were used in this study. For dark-rearing experiments, mothers with P0 or P20 litters were placed for 7 days in a light-tight container in which temperature, humidity, and luminance were continually monitored (Hooks and Chen, 2006). Control (normally light reared, LR) animals were raised under a 12 hr light/dark cycle. For cortical neurons cultures, pregnant Wistar rats were used. All the procedures were reviewed and approved by the IACUC at Children's Hospital, Boston or by DGAV, Portugal.

Electrophysiology

Acute LGN brain slices and the electrophysiological methods used to study development of the retinogeniculate synapse have been described previously (Chen and Regehr, 2000; Hooks and Chen, 2006, 2008). Peak single fiber AMPAR EPSC amplitudes were obtained from minimal stimulation (Chen and Regehr, 2000). Single fiber measurements included a second input from a given cell if it was recruited during incremental increase in stimulus intensity (0.25 μA) and clearly resolvable (5× greater in amplitude) from the first input. Details in Supplemental Information.

Immunocytochemistry

Low-density rat cortical neurons were fixed in 4% paraformaldehyde and incubated with the following antibodies: stargazin (Abcam, ab64237), PSD95 (Thermo Scientific, MA1-045) and Map2 (Abcam, ab5392), as previously described in (Santos et al., 2012). For cell-surface staining of GluA1, anti-GluA1 N-terminal antibody was added to neurons for 10 min at room temperature, washed, and neurons were fixed as above. For details see Supplemental Information.

NIH-PA Author Manuscript

NIH-PA Author Manuscript

NIH-PA Author Manuscript

Western blot

High-density rat cortical neurons were lysed with TEEN buffer: 25 mM Tris-Cl, pH 7.4, 1 mM EDTA, 1 mM EGTA, 150 mM NaCl and 1% Triton X-100 supplemented with protease and phosphatase inhibitors. The following Merck Millipore antibodies were used: anti-stargazin (AB9876), anti-phospho stargazin (Ser239/Ser240) (AB3713), anti-phospho stargazin (Ser228) (AB15435), anti-GluA1 (AB1504), anti-GluA2 (MAB397).

Statistical Analysis

Normality of current amplitude distributions was tested by comparison to a theoretical normal distribution using a Kolmogorov-Smirnov test. Statistical significance was tested using Kruskal-Wallis or Mann-Whitney tests as maximal current and single fiber current values were typically not normally distributed. Biochemical and immunocytochemical data are presented as mean ± SEM of at least three different experiments, performed in independent preparations. Statistical analysis of the results was performed using either paired student t-test or one-way or two-way ANOVA analysis followed by either Dunnett's or Bonferroni post test: n.s. non significant, ***P<0.001, **P<0.01, *P<0.05.

Supplementary Material

Refer to Web version on PubMed Central for supplementary material.

Acknowledgments

Susana R. Louros was supported by FCT, Portugal. This work was supported by FCT and FEDER, Portugal (PEst-C/SAU/LA0001/2013–2014, PTDC/SAU-NEU/099440/2008 and PTDC/NEU-NCM/0750/2012 to ALC), NIH F31 NS048630 (to BMH.), NIH EY013613 and HD018655 (to CC). We thank the Greenberg lab for assistance in designing the shRNA#4, Dr. S. Tomita (University of Yale, USA) for the kind gift of STG phosphomutant constructs, and Dr. Andrew Irving (University of Dundee, UK) for the GluA1 N-terminus antibody. We are grateful to C.B. Duarte, A. Thompson, J. Hauser, J. Leffler, M.E. Greenberg and T. Schwarz for critical reading of the manuscript. We also thank E. Carvalho for assistance in the preparation of cultured neurons and the MICC imaging facility.

References

Anggono V, Clem RL, Huganir RL. PICK1 loss of function occludes homeostatic synaptic scaling. J Neurosci. 2011; 31:2188–2196. [PubMed: 21307255]

Arendt KL, Sarti F, Chen L. Chronic inactivation of a neural circuit enhances LTP by inducing silent synapse formation. J Neurosci. 2013; 33:2087–2096. [PubMed: 23365245]

Bats C, Groc L, Choquet D. The interaction between Stargazin and PSD-95 regulates AMPA receptor surface trafficking. Neuron. 2007; 53:719–734. [PubMed: 17329211]

Bats C, Soto D, Studniarczyk D, Farrant M, Cull-Candy SG. Channel properties reveal differential expression of TARPed and TARPless AMPARs in stargazer neurons. Nature neuroscience. 2012; 15:853–861.

Blackman MP, Djukic B, Nelson SB, Turrigiano GG. A critical and cell-autonomous role for MeCP2 in synaptic scaling up. J Neurosci. 2012; 32:13529–13536. [PubMed: 23015442]

Burgess DL, Noebels JL. Single gene defects in mice: the role of voltage-dependent calcium channels in absence models. Epilepsy Res. 1999; 36:111–122. [PubMed: 10515159]

Butts DA, Kanold PO, Shatz CJ. A burst-based "Hebbian" learning rule at retinogeniculate synapses links retinal waves to activity-dependent refinement. PLoS Biol. 2007; 5:e61. [PubMed: 17341130]

NIH-PA Author Manuscript

NIH-PA Author Manuscript

NIH-PA Author Manuscript

Chandrasekaran AR, Plas DT, Gonzalez E, Crair MC. Evidence for an instructive role of retinal activity in retinotopic map refinement in the superior colliculus of the mouse. J Neurosci. 2005; 25:6929–6938. [PubMed: 16033903]

Chandrasekaran AR, Shah RD, Crair MC. Developmental homeostasis of mouse retinocollicular synapses. J Neurosci. 2007; 27:1746–1755. [PubMed: 17301182]

Chen C, Regehr WG. Developmental remodeling of the retinogeniculate synapse. Neuron. 2000; 28:955–966. [PubMed: 11163279]

Chen L, Chetkovich DM, Petralia RS, Sweeney NT, Kawasaki Y, Wenthold RJ, Bredt DS, Nicoll RA. Stargazin regulates synaptic targeting of AMPA receptors by two distinct mechanisms. Nature. 2000; 408:936–943. [PubMed: 11140673]

Desai NS, Cudmore RH, Nelson SB, Turrigiano GG. Critical periods for experience-dependent synaptic scaling in visual cortex. Nature neuroscience. 2002; 5:783–789.

Fukaya M, Yamazaki M, Sakimura K, Watanabe M. Spatial diversity in gene expression for VDCC gamma subunit family in developing and adult mouse brains. Neuroscience research. 2005; 53:376–383. [PubMed: 16171881]

Goel A, Jiang B, Xu LW, Song L, Kirkwood A, Lee HK. Cross-modal regulation of synaptic AMPA receptors in primary sensory cortices by visual experience. Nature neuroscience. 2006; 9:1001–1003.

Groth RD, Lindskog M, Thiagarajan TC, Li L, Tsien RW. Beta Ca2+/CaM-dependent kinase type II triggers upregulation of GluA1 to coordinate adaptation to synaptic inactivity in hippocampal neurons. Proceedings of the National Academy of Sciences of the United States of America. 2011; 108:828–833. [PubMed: 21187407]

He HY, Ray B, Dennis K, Quinlan EM. Experience-dependent recovery of vision following chronic deprivation amblyopia. Nature neuroscience. 2007; 10:1134–1136.

Hollmann M, Hartley M, Heinemann S. Ca2+ permeability of KA-AMPA-gated glutamate receptor channels depends on subunit composition. Science. 1991; 252:851–853. [PubMed: 1709304]

Hong YK, Chen C. Wiring and rewiring of the retinogeniculate synapse. Current opinion in neurobiology. 2011; 21:228–237. [PubMed: 21558027]

Hooks BM, Chen C. Distinct roles for spontaneous and visual activity in remodeling of the retinogeniculate synapse. Neuron. 2006; 52:281–291. [PubMed: 17046691]

Hooks BM, Chen C. Vision triggers an experience-dependent sensitive period at the retinogeniculate synapse. J Neurosci. 2008; 28:4807–4817. [PubMed: 18448657]

Jackson AC, Nicoll RA. The expanding social network of ionotropic glutamate receptors: TARPs and other transmembrane auxiliary subunits. Neuron. 2011; 70:178–199. [PubMed: 21521608]

Kaneko M, Stellwagen D, Malenka RC, Stryker MP. Tumor necrosis factor-alpha mediates one component of competitive, experience-dependent plasticity in developing visual cortex. Neuron. 2008; 58:673–680. [PubMed: 18549780]

Kielland A, Bochorishvili G, Corson J, Zhang L, Rosin DL, Heggelund P, Zhu JJ. Activity patterns govern synapse-specific AMPA receptor trafficking between deliverable and synaptic pools. Neuron. 2009; 62:84–101. [PubMed: 19376069]

Krahe TE, Guido W. Homeostatic plasticity in the visual thalamus by monocular deprivation. J Neurosci. 2011; 31:6842–6849. [PubMed: 21543614]

Lacey CJ, Bryant A, Brill J, Huguenard JR. Enhanced NMDA receptor-dependent thalamic excitation and network oscillations in stargazer mice. J Neurosci. 2012; 32:11067–11081. [PubMed: 22875939]

Lee HK. Ca-permeable AMPA receptors in homeostatic synaptic plasticity. Frontiers in molecular neuroscience. 2012; 5:17. [PubMed: 22347846]

Lisman J, Yasuda R, Raghavachari S. Mechanisms of CaMKII action in long-term potentiation. Nat Rev Neurosci. 2012; 13:169–182. [PubMed: 22334212]

Maffei A, Turrigiano G. The age of plasticity: developmental regulation of synaptic plasticity in neocortical microcircuits. Progress in brain research. 2008; 169:211–223. [PubMed: 18394476]

Malinow R, Madison DV, Tsien RW. Persistent protein kinase activity underlying long-term potentiation. Nature. 1988; 335:820–824. [PubMed: 2847049]

NIH-PA Author Manuscript

NIH-PA Author Manuscript

NIH-PA Author Manuscript

Matsuda S, Kakegawa W, Budisantoso T, Nomura T, Kohda K, Yuzaki M. Stargazin regulates AMPA receptor trafficking through adaptor protein complexes during long-term depression. Nat Commun. 2013; 4:2759. [PubMed: 24217640]

Menuz K, Nicoll RA. Loss of inhibitory neuron AMPA receptors contributes to ataxia and epilepsy in stargazer mice. J Neurosci. 2008; 28:10599–10603. [PubMed: 18923036]

Mrsic-Flogel TD, Hofer SB, Ohki K, Reid RC, Bonhoeffer T, Hubener M. Homeostatic regulation of eye-specific responses in visual cortex during ocular dominance plasticity. Neuron. 2007; 54:961–972. [PubMed: 17582335]

Nicoll RA, Roche KW. Long-term potentiation: Peeling the onion. Neuropharmacology. 2013

Noutel J, Hong YK, Leu B, Kang E, Chen C. Experience-dependent retinogeniculate synapse remodeling is abnormal in MeCP2-deficient mice. Neuron. 2011; 70:35–42. [PubMed: 21482354]

Ohara PT, Lieberman AR, Hunt SP, Wu JY. Neural elements containing glutamic acid decarboxylase (GAD) in the dorsal lateral geniculate nucleus of the rat; immunohistochemical studies by light and electron microscopy. Neuroscience. 1983; 8:189–211. [PubMed: 6341876]

Opazo P, Labrecque S, Tigaret CM, Frouin A, Wiseman PW, De Koninck P, Choquet D. CaMKII triggers the diffusional trapping of surface AMPARs through phosphorylation of stargazin. Neuron. 2010; 67:239–252. [PubMed: 20670832]

Payne HL. The role of transmembrane AMPA receptor regulatory proteins (TARPs) in neurotransmission and receptor trafficking (Review). Molecular membrane biology. 2008; 25:353–362. [PubMed: 18446621]

Qiu Z, Sylwestrak EL, Lieberman DN, Zhang Y, Liu XY, Ghosh A. The Rett syndrome protein MeCP2 regulates synaptic scaling. J Neurosci. 2012; 32:989–994. [PubMed: 22262897]

Santos SD, Iuliano O, Ribeiro L, Veran J, Ferreira JS, Rio P, Mulle C, Duarte CB, Carvalho AL. Contactin-associated Protein 1 (Caspr1) Regulates the Traffic and Synaptic Content of alpha-Amino-3-hydroxy-5-methyl-4-isoxazolepropionic Acid (AMPA)-type Glutamate Receptors. The Journal of biological chemistry. 2012; 287:6868–6877. [PubMed: 22223644]

Schnell E, Sizemore M, Karimzadegan S, Chen L, Bredt DS, Nicoll RA. Direct interactions between PSD-95 and stargazin control synaptic AMPA receptor number. Proceedings of the National Academy of Sciences of the United States of America. 2002; 99:13902–13907. [PubMed: 12359873]

Soto D, Coombs ID, Kelly L, Farrant M, Cull-Candy SG. Stargazin attenuates intracellular polyamine block of calcium-permeable AMPA receptors. Nature neuroscience. 2007; 10:1260–1267.

Sumioka A, Yan D, Tomita S. TARP phosphorylation regulates synaptic AMPA receptors through lipid bilayers. Neuron. 2010; 66:755–767. [PubMed: 20547132]

Thiagarajan TC, Piedras-Renteria ES, Tsien RW. alpha- and betaCaMKII. Inverse regulation by neuronal activity and opposing effects on synaptic strength. Neuron. 2002; 36:1103–1114. [PubMed: 12495625]

Tomita S, Chen L, Kawasaki Y, Petralia RS, Wenthold RJ, Nicoll RA, Bredt DS. Functional studies and distribution define a family of transmembrane AMPA receptor regulatory proteins. J Cell Biol. 2003; 161:805–816. [PubMed: 12771129]

Tomita S, Stein V, Stocker TJ, Nicoll RA, Bredt DS. Bidirectional synaptic plasticity regulated by phosphorylation of stargazin-like TARPs. Neuron. 2005; 45:269–277. [PubMed: 15664178]

Turrigiano GG. The self-tuning neuron: synaptic scaling of excitatory synapses. Cell. 2008; 135:422–435. [PubMed: 18984155]

Turrigiano GG, Leslie KR, Desai NS, Rutherford LC, Nelson SB. Activity-dependent scaling of quantal amplitude in neocortical neurons. Nature. 1998; 391:892–896. [PubMed: 9495341]

Wierenga CJ, Ibata K, Turrigiano GG. Postsynaptic expression of homeostatic plasticity at neocortical synapses. J Neurosci. 2005; 25:2895–2905. [PubMed: 15772349]

Yamazaki M, Fukaya M, Hashimoto K, Yamasaki M, Tsujita M, Itakura M, Abe M, Natsume R, Takahashi M, Kano M, et al. TARPs gamma-2 and gamma-7 are essential for AMPA receptor expression in the cerebellum. Eur J Neurosci. 2010; 31:2204–2220. [PubMed: 20529126]

Zhong X, Li H, Chang Q. MeCP2 phosphorylation is required for modulating synaptic scaling through mGluR5. J Neurosci. 2012; 32:12841–12847. [PubMed: 22973007]

Ziburkus J, Dilger EK, Lo FS, Guido W. LTD and LTP at the developing retinogeniculate synapse. Journal of neurophysiology. 2009; 102:3082–3090. [PubMed: 19776360]

NIH-PA Author Manuscript

NIH-PA Author Manuscript

NIH-PA Author Manuscript

NIH-PA Author Manuscript

NIH-PA Author Manuscript

NIH-PA Author Manuscript

Highlights

- Vision regulates stargazin levels and phosphorylation at the retinogeniculate synapse
- Stargazin mediates experience-dependent remodeling of the retinogeniculate synapse
- Stargazin is essential for synaptic scaling
- Stargazin phosphorylation mediates homeostatic plasticity

NIH-PA Author Manuscript
NIH-PA Author Manuscript
NIH-PA Author Manuscript

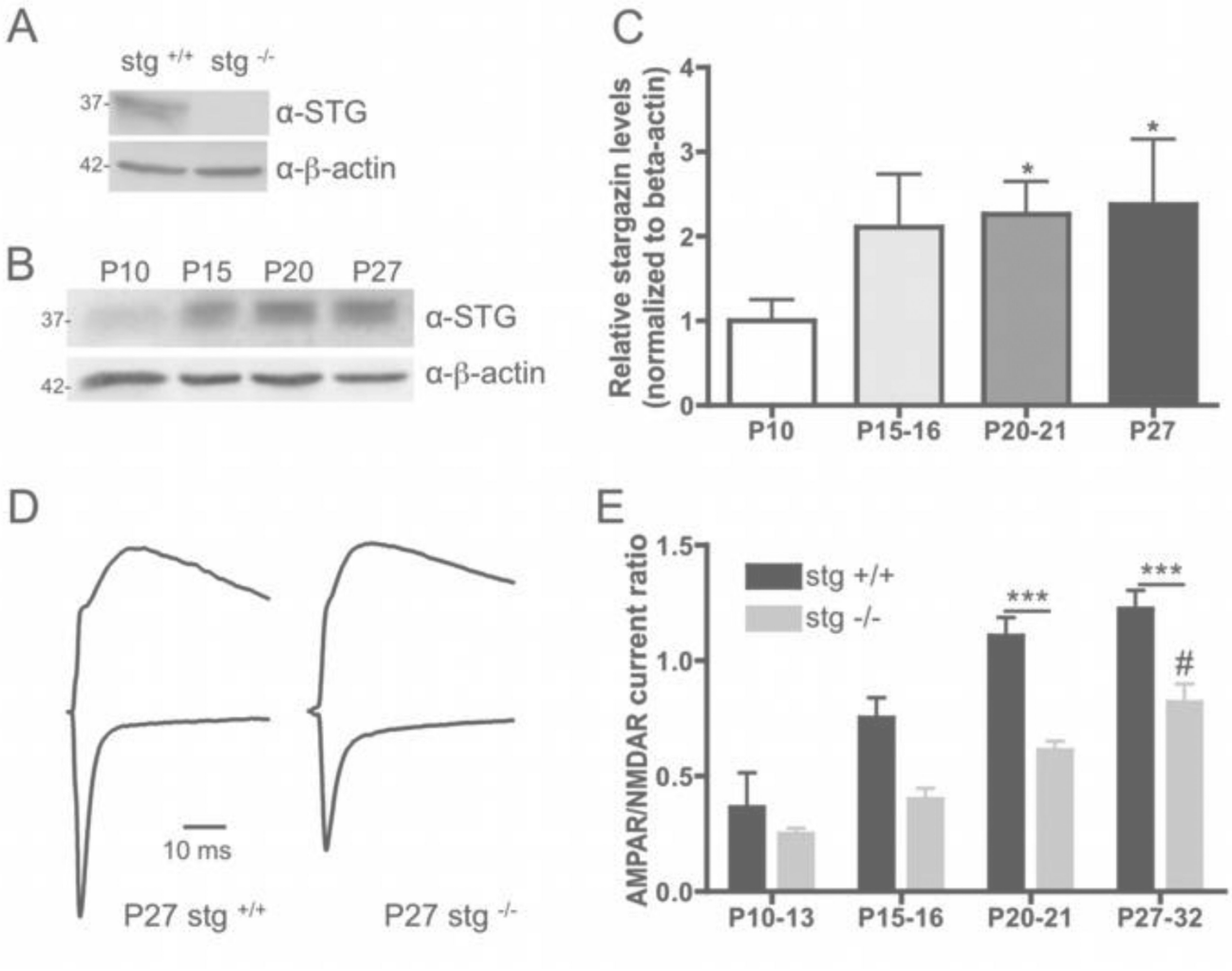

Fig. 1. STG is important for AMPAR trafficking in the retinogeniculate synapse

Representative western blot from LGN of P27 stg+/+ and stg −/− mice showing that the STG antibody used in this study is specific. (B) Representative western blot against total STG in mouse LGNs at different developmental ages. (C) STG levels significantly increase after eyeopening and remain high up to P27 (N=4, t-test, *P<0.05). (D) Representative synaptic recordings from P27 stg−/− and stg+/+ mice. Superimposed glutamatergic AMPAR and NMDAR currents were evoked at HP=−70 mV (inward currents) and +40 mV (outward currents), respectively. Currents are normalized to the peak NMDAR current amplitude. (E) Comparison of the average peak AMPAR/NMDAR current ratio over development in stg−/− and stg+/+ littermates. stg−/− (P11–13): 13 cells from 6 animals; (P15–16): 26 from 9; (P20–21) 23 from 15; (P27–32): 38 from 23. stg+/+ (P11–13) 9 from 2 (P15–16): 19 cells from 6 animals; (P20–21) 21 from 10; (P27–32): 36 from 23. (ANOVA, Bonferroni test,***P<0.001 stg−/− vs. WT; # P<0.01 stg−/− P27–32 vs. stg−/− P15). See also Figure S1.

NIH-PA Author Manuscript
NIH-PA Author Manuscript
NIH-PA Author Manuscript

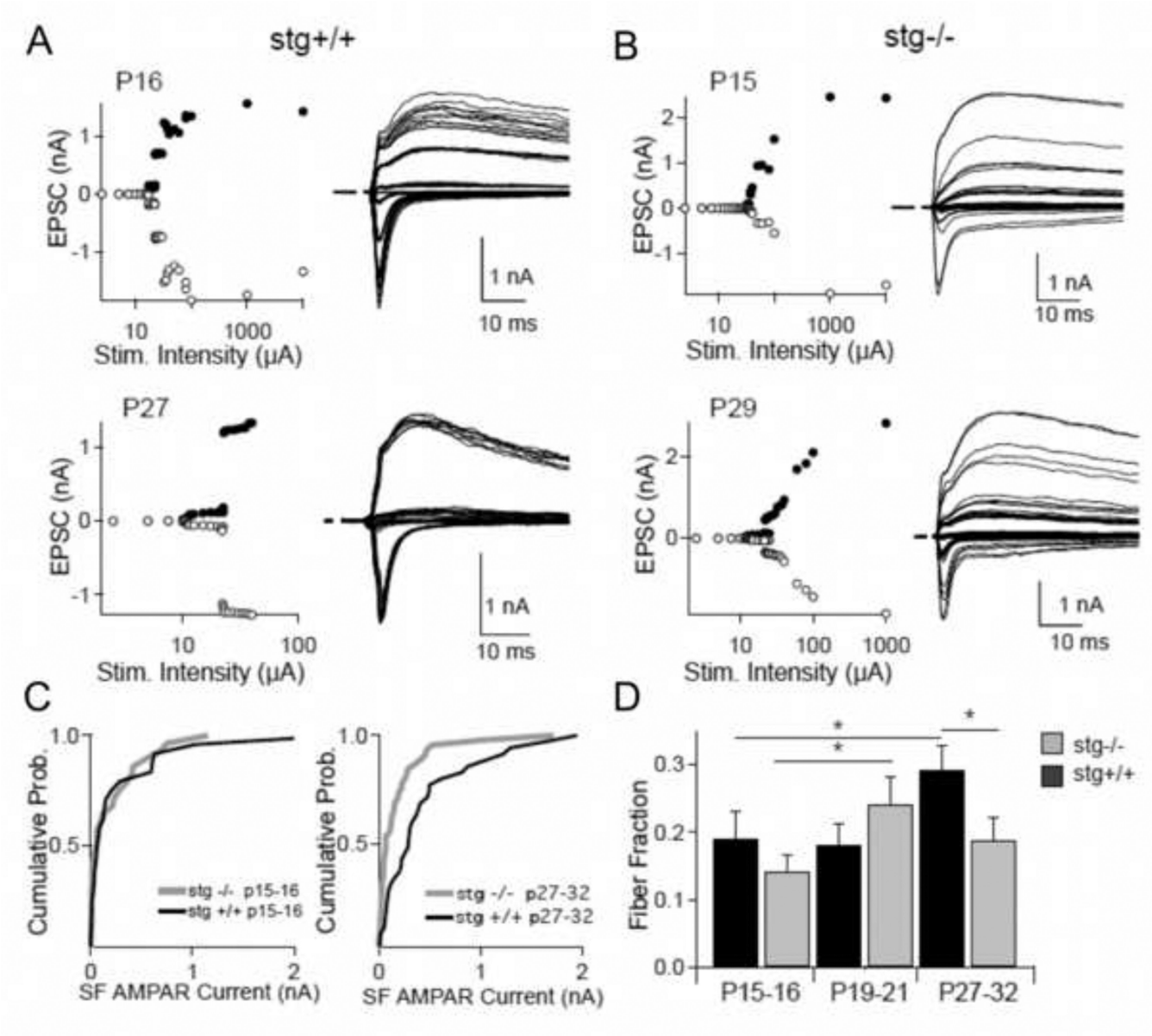

Fig. 2. STG is important for the late phase of retinogeniculate synapse refinement

Representative recordings from stg+/+ (A) and stg−/− (B) littermates at P15–16 (top panels) and P27–32 (lower panels). For each example, (*Left*) plot of the peak EPSC amplitude (nA) vs. stimulus intensity for both AMPAR (white circles) and NMDAR mediated (black circles) components of the synaptic current. (*Right*) Superimposed EPSCs recorded from the same relay neuron at −70 mV (inward currents) or +40 mV (outward currents) while increasing the stimulus intensity. (C) Comparison of single fiber (SF) AMPAR current amplitude cumulative probability histograms for stg−/− and stg+/+ littermates during the spontaneous activity dependent (P15–16) and experience-dependent (P27–32) phases of synaptic remodeling (n=24 to 45). stg−/− is significantly different from their stg+/+ littermates at P27–32, but not at P15–16, Mann-Whitney. (D) Comparison of fiber fraction over development (*P<0.05, by 1-way ANOVA, Kruskal-Wallis test with Dunn's multiple

comparison, n=48–93). A higher fiber fraction indicates fewer afferent inputs and more a refined circuit. See also Figure S2.

NIH-PA Author Manuscript

NIH-PA Author Manuscript

NIH-PA Author Manuscript

NIH-PA Author Manuscript

NIH-PA Author Manuscript

NIH-PA Author Manuscript

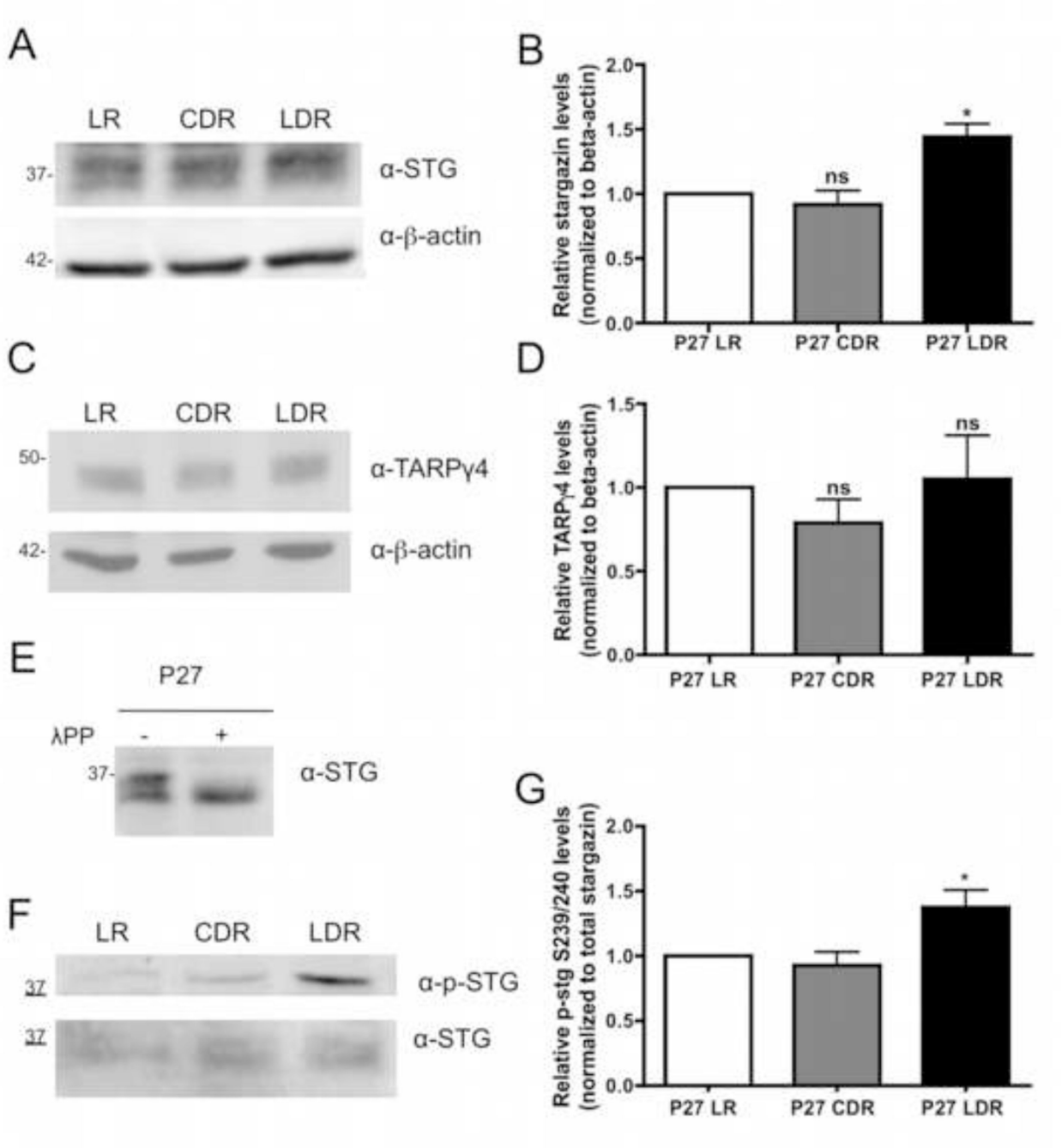

Fig. 3. Visual experience alters STG expression and phosphorylation in the LGN

Representative western blot of mouse LGNs (P27) comparing the effects of CDR and LDR on (A) STG and (C) TARPγ4 expression levels. Quantification of average normalized STG (B, N=4) and TARPγ4 (D, N= 3) levels in CDR and LDR. (E) Effects of lambda-phosphatase on STG mobility in P27 LGN. (F, G) Comparison of STG phosphorylation at S239/240 in the LGN of LR, CDR and LDR P27 mice. (N=3) ANOVA, Dunnett's test, * $P<0.05$ for all the panels in this figure. See also Figure S3.

NIH-PA Author Manuscript
NIH-PA Author Manuscript
NIH-PA Author Manuscript

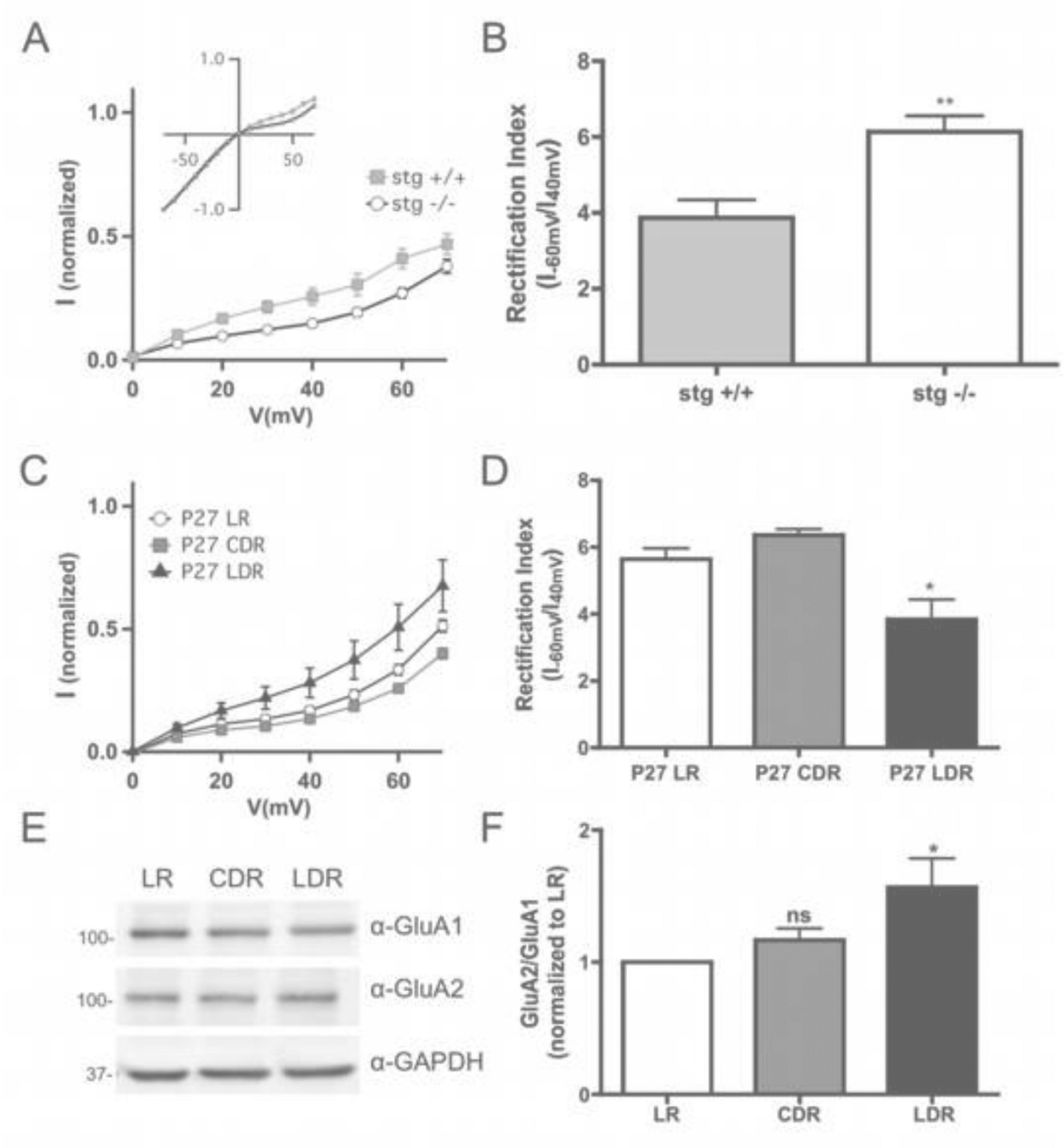

Fig. 4. AMPAR composition in experience-dependent retinogeniculate plasticity

(A) AMPAR I-Vs normalized to the current amplitude at −70 mV for stg +/+ and stg −/− mice. Currents recorded in the presence of R-CPP and bicuculline in the bath and spermine in the intracellular solution. I-V relationship is shown between 0 and +70 mV with full I-V range shown in inset. (B) Average RI, stg+/+ vs. stg−/− (N=8 stg+/+; N=10 stg−/−; P=0.002, t-test). (C) Normalized I-Vs for C57 mice that have experienced different sensory manipulations. (D) Average RI in visually manipulated mice (N=4, <0.05, ANOVA, Bonferroni test, LDR vs. LR). (E) AMPA receptor subunits GluA1 and GluA2 were

analyzed from whole LGN lysates. (F) Relative abundance of these subunits plotted as GluA1/GluA2 ratio (N=3, ANOVA, Dunnett's test, * $P<0.05$, LDR vs. LR).

NIH-PA Author Manuscript
NIH-PA Author Manuscript
NIH-PA Author Manuscript

NIH-PA Author Manuscript

NIH-PA Author Manuscript

NIH-PA Author Manuscript

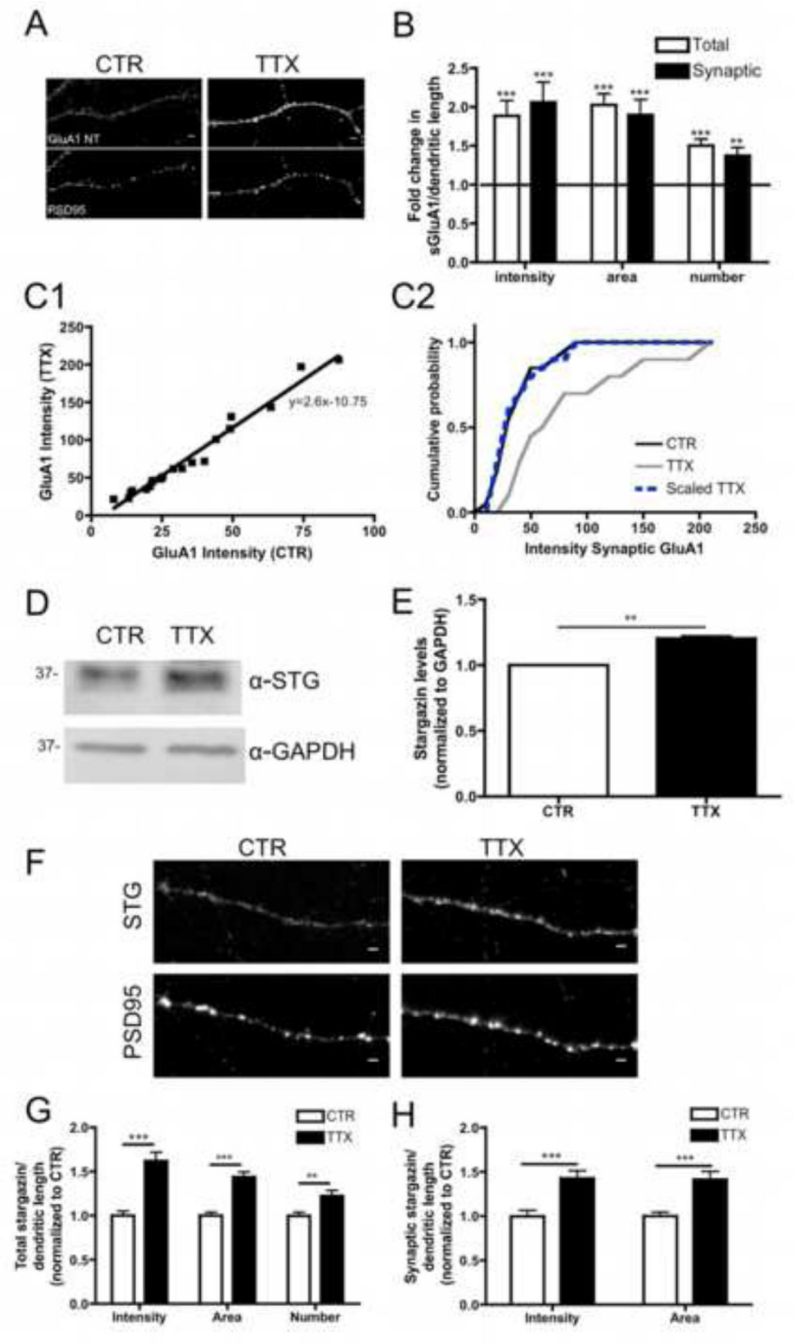

Fig. 5. STG is increased in cortical neurons by TTX-induced synaptic scaling

(A) Representative examples of surface GluA1 *(top)* and PSD95 *(bottom)* labeling. (B) Both total and synaptic surface GluA1 levels were significantly increased by TTX incubation, N=30 cells each condition, t-test,***P<0.0001 **P<0.001 compared to CTR. (C1) Ranked CTR intensities were plotted against ranked TTX intensities, and the best-fit function was determined. (C2) Cumulative distributions of CTR (black) and TTX (grey) synaptic surface GluA1 intensities. The original TTX distribution was transformed by the best-fit equation and plotted (dashed line). (D) Cortical neurons whole-cell lysates probed with anti-STG and

anti-GAPDH antibodies. (E) Average total STG levels increased by 20.3 ± 2% of control after TTX incubation (N=3, t-test, P=0.009 vs. CTR). (F) TTX treatment significantly increased total (G) and synaptic (H) STG puncta (intensity, area and number; N=30 cells each condition, t-test, *** P<0.0001 vs. CTR).

NIH-PA Author Manuscript
NIH-PA Author Manuscript
NIH-PA Author Manuscript

NIH-PA Author Manuscript

NIH-PA Author Manuscript

NIH-PA Author Manuscript

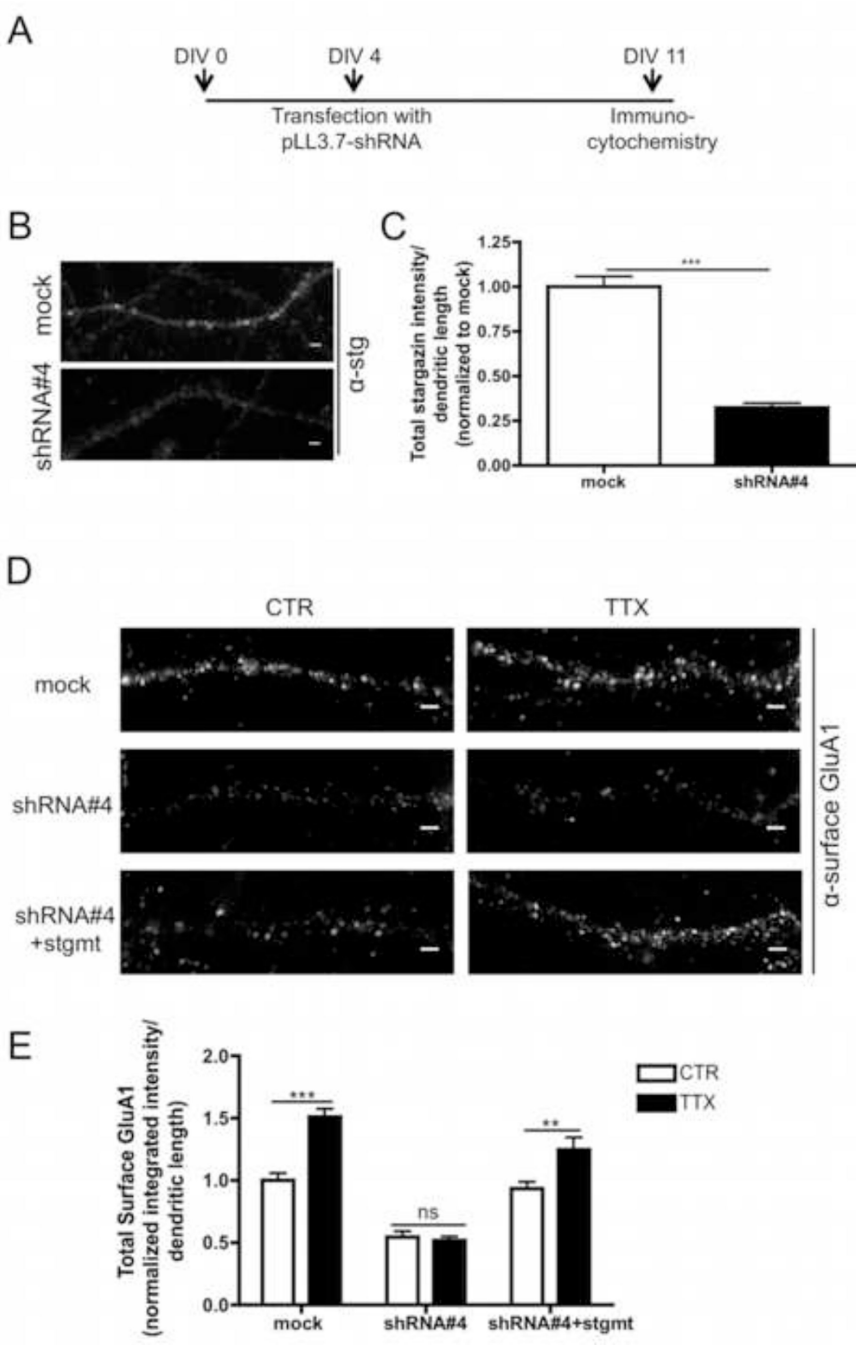

Fig. 6. STG is essential for synaptic scaling

(A) Cortical neurons were transfected with pLL-mock or pLL-shRNA#4 and total levels of STG were analyzed by immunocytochemistry after 7 days of transfection. (B) Representative images of STG distribution in transfected DIV11 cortical neurons and (C) quantification of total intensity of STG puncta demonstrated efficient knockdown of the protein by shRNA#4 (32.2 ± 3% of mock, N=27 cells each condition, P=0.001, t-test). (D,E) Quantification of surface GluA1 immunocytochemistry comparing total surface intensity of GluA1 clusters. Normal increase in GluA1 intensity in response to TTX treatment was

NIH-PA Author Manuscript

NIH-PA Author Manuscript

NIH-PA Author Manuscript

blocked in neurons transfected with shRNA#4 but not in neurons transfected with shRNA#4 and a STG mutant refractory to this shRNA (N=26 cells each condition, from three independent experiments; **P<0.01; ***P<0.001, ANOVA, Bonferroni test, TTX compared to CTR).

NIH-PA Author Manuscript
NIH-PA Author Manuscript
NIH-PA Author Manuscript

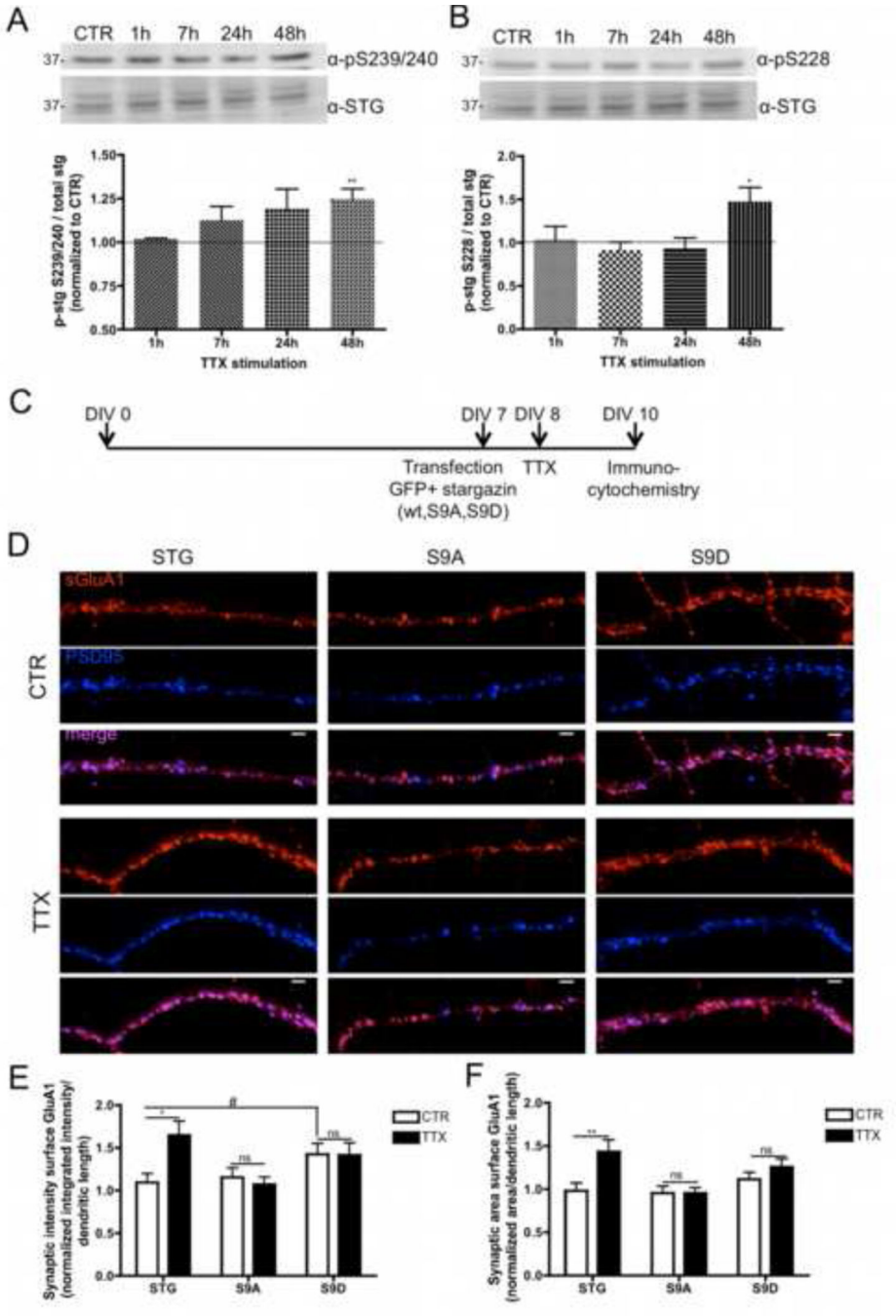

Fig. 7. STG phosphorylation is required for synaptic scaling

(A) Changes in the phosphorylation of STG after TTX treatment for 1 to 48h. STG phosphorylation at S239/240 increased after 7h of activity blockade and is significantly increased after 48h TTX stimulation (N=4 independent preparations, 24.7±5.8% compared to CTR, P=0.005, t-test). (B) STG phosphorylation at S228 was significantly increased after 48h of activity blockade (N=4 independent preparations, 47.4±16% compared to CTR, P=0.031, t-test). (C) Cortical neurons were transfected with WT stargazin, phospho-dead stargazin (S9A) or phospho-mimetic stargazin (S9D) along with GFP and stimulated with

NIH-PA Author Manuscript

NIH-PA Author Manuscript

NIH-PA Author Manuscript

TTX. (D) Surface GluA1 (red) and PSD95 (blue) were analyzed by immunocytochemistry. (E,F) Activity blockade induced an increase in synaptic surface GluA1 intensity and area in WT stargazin-transfected neurons, but over-expression of S9A or S9D mutant forms of stargazin blocked TTX induced GluA1 accumulation at the surface and synaptic sites. (red – surface GluA1; blue -PSD95; magenta: surface GluA1 colocalized with PSD95). N=26 cells each condition. (** $P<0.01$, * $P<0.05$, significantly different from CTR; # $p<0.05$, S9D CTR significantly different from STG CTR, 2-way ANOVA, Bonferroni test). See also Figures S4 and S5.